Protein Cell, 2025, **16**, 822–828
https://doi.org/10.1093/procel/pwaf016
Advance access publication 11 June 2025
Letter

Protein & Cell

Letter

Lamin C conserves DNA replication factors via phase separation during oxidative stress for DNA replication recovery

Mingkang Jia[1], Gan Zhao[1], Mengjie Sun[1], Xiangyang Wang[1], He Ren[1], Guangwei Xin[1], Qing Jiang[1], Chuanmao Zhang[1,2,*]

[1]The Key Laboratory of Cell Proliferation and Differentiation of the Ministry of Education, School of Life Sciences, Peking University, Beijing 100871, China
[2]The Academy for Cell and Life Health, Faculty of Life Science and Technology, Kunming University of Science and Technology, Kunming 650500, China

*Correspondence: zhangcm@kust.edu.cn or zhangcm@pku.edu.cn (C. Zhang)

Dear Editor,

Excessive reactive oxygen species (ROS) cause damage to biomolecules and lead to DNA replication fork slowdown and even stalling (Sies and Jones, 2020; Somyajit et al., 2017; Wilhelm et al., 2016); this state is referred to as oxidative stress. Eukaryotic cells employ diverse strategies to maintain redox homeostasis, including the formation of biomolecular condensates through phase separation. In mussels, for example, Catecholic 3,4-dihydroxyphenyl-L-alanine (Dopa)-containing mussel foot protein 3 and mussel foot protein 6 form redox insulators via phase separation to protect DOPA from oxidation (Valois et al., 2020). In mammalian cells, oxidative stress induces the assembly of stress granules through the phase separation of mRNAs and mRNA-associated proteins to improve cell survival (Guillén-Boixet et al., 2020; Wang et al., 2021).

Lamins are the main components of the nuclear lamina (NL) beneath the nuclear envelope in metazoan cells. In mammalian somatic cells, lamins are categorized into two types: the A-type, which comprises lamin A and lamin C, and the B-type, which includes lamin B1 and lamin B2 (Burke and Stewart, 2013). Several studies have reported that the overexpression of wild-type (WT) lamin C or mutants of lamin A, lamin C, or lamin B1 results in the formation of lamin protein condensates (Izumi et al., 2000; Sylvius et al., 2005, 2008). These condensates are regarded as nonfunctional protein aggregates that may lead to disease.

In this work, we found that endogenous lamin A/C could form nuclear protein condensates in response to H_2O_2-induced oxidative stress (Fig. 1A). We also observed that, in cells stably expressing low levels of green fluorescent protein (GFP)-lamin A (GLA) or GFP-lamin C (GLC) under oxidative stress, both the GLC and GLA proteins could form nuclear protein condensates, whereas GFP alone could not (Figs. 1B and S1). By quantifying the number of cells exhibiting lamin condensates under oxidative stress, we revealed that a significantly greater proportion of the cells formed GLC condensates than formed GLA condensates (Fig. 1C). Hence, we focused on the lamin C condensates afterward.

We first established a lamin C-mClover (LCmC) knock-in HeLa cell line, named lamin A knockout (LAO)-LCmC, to elucidate the properties and functions of the lamin C condensates (Fig. S2). LAO-LCmC cells express endogenous lamin C, which is tagged with a GFP variant mClover, but it lacks the expression of lamin A, potentially due to altered alternative splicing of the *LMNA* gene following gene editing (Fig. S2C). Upon exposure to oxidative stress, the LCmC proteins in LAO-LCmC cells were also induced to assemble into lamin C condensates (Fig. 1D and 1E). In addition to exogenous H_2O_2, the intracellular ROS generated by treating cells

Accepted 6 February 2025.

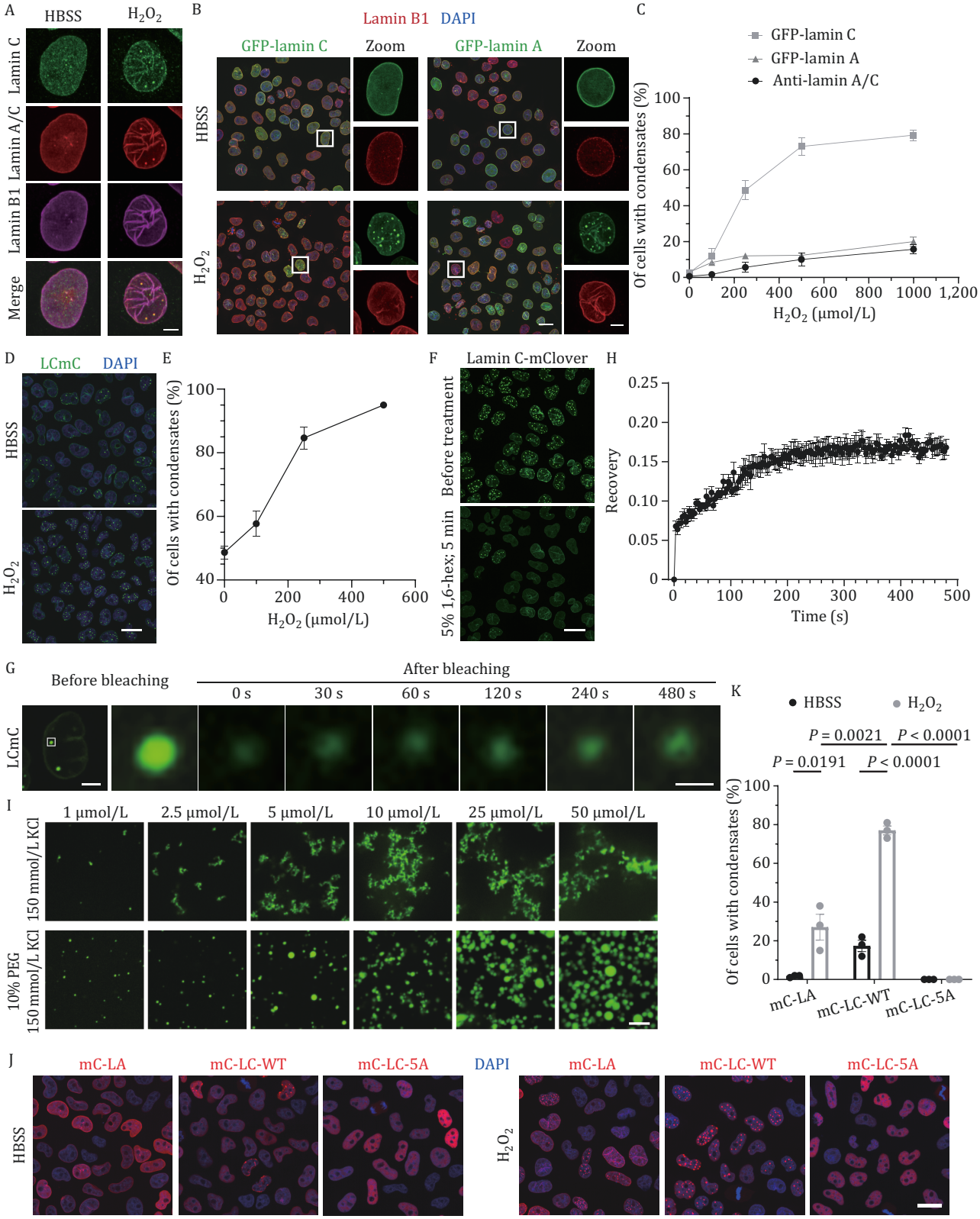

Figure 1. Lamin C proteins assemble into condensates by phase separation during oxidative stress. (A) Representative images of WT HeLa cells treated with 250 μmol/L H_2O_2 or HBSS for 60 min. WT HeLa cells were costained with anti-lamin C, anti-lamin A/C, and anti-lamin B1 antibodies. Scale bar, 5 μm. (B) Representative images of cells stably expressing GLA and GLC and treated with 250 μmol/L H_2O_2 or HBSS for 60 min. The cells were costained with an anti-lamin B1 antibody (red) and DAPI (blue). Scale bars, 20 μm and 5 μm (zoom). (C) Quantification of the frequency of WT HeLa cells and stable GLA- and GLC-expressing cells with lamin condensates under the indicated conditions. The data are presented as the mean ± SEM from three independent experiments. One hundred cells were counted per sample in each experiment. (D) Representative images of LAO-LCmC cells treated with 250 μmol/L H_2O_2 or HBSS for 40 min. Scale bar, 20 μm. (E) Quantification of the frequency of LAO-LCmC cells with lamin condensates under the indicated conditions. The data are presented as the mean ± SEM from three independent experiments. One hundred cells were counted per

with menadione, a compound that generates oxidants through redox cycling in cells (Thor et al., 1982), also induced the assembly of lamin C condensates (Fig. S3A). We determined whether oxidative stress was unique in inducing the formation of lamin C condensates by testing several other stresses/conditions. We found that all these stresses/conditions failed to induce the formation of lamin C condensates (Fig. S3A). We further revealed that the oxidative stress-induced lamin C condensates did not contain any markers of the nuclear bodies that we tested (Fig. S3B). Overall, we conclude that lamin C condensates are newly recognized nuclear bodies and that their formation is a specific response to oxidative stress. Hence, we designate the lamin C condensate as the "lamin C body."

We speculated that the lamin C bodies were formed by phase separation. We found that GLA or GLC bodies formed by transient overexpression and LCmC bodies induced by oxidative stress were both dissolved by the treatment of cells with 1,6-hexanediol (Figs. 1F and S4A), a compound known to disrupt liquid-like bodies formed by phase separation. Through a fluorescence recovery after photobleaching (FRAP) assay, we revealed that, after photobleaching, the fluorescence intensity of the GLA and GLC bodies recovered by approximately 42% and 52%, respectively, indicating that they possess liquid-like properties (Fig. S4B and S4C), whereas the fluorescence intensity of the LCmC bodies induced by oxidative stress recovered by approximately 18%, indicating that the oxidative stress-induced endogenous lamin C bodies possess gel-like properties (Fig. 1G and 1H). We subsequently performed an *in vitro* phase separation assay. Because full-length lamin C proteins easily precipitate *in vitro*, likely because of their coiled-coil domains, we overexpressed a series of lamin C truncates lacking a partial coiled-coil domain in *LMNA*-knockout (KO) HeLa cells to identify a truncated protein suitable for *in vitro* phase separation assays (Figs. S5 and S6A). As a result, the Δ1BΔ2B59 truncated protein could assemble into lamin condensates in cells (Fig. S6A–C). The purified Δ1BΔ2B59 protein could form droplet-like condensates at various concentrations, including at micromolar physiological concentrations, in physiological saline buffer with 10% polyethylene glycol (PEG) (Figs. 1I and S6D). Collectively, these data indicate that, under oxidative stress, lamin C assembles condensates through phase separation.

We transiently overexpressed several lamin truncations in cells to identify the essential domains within the lamin C molecule that facilitate phase separation (Fig. S7A). The results revealed that the truncations lacking the rod domain (Head-nuclear localization signal (NLS), NLS-Ig-like, GLC-NLS-C, and GLA-NLS-C) and the truncations lacking the head domain (GLA-ΔHead and GLC-ΔHead) failed to undergo phase separation, whereas the C-terminus deletion truncate (ΔC) retained the phase separation ability, indicating that both the rod domain and the head domain are essential for phase separation of the lamin proteins (Fig. S7). We noted that five amino acids with positive charges within the head domain are highly conserved (Fig. S8A). Eliminating these positive charges through the mutation of these arginines to alanines in GLC (GLC-5A) largely reduced its ability to form condensates (Fig. S8B and S8C). We also established several cell lines (mCL cells) stably expressing mCherry-lamin A (mC-LA), mCherry-lamin C-WT (mC-LC-WT) or mCherry-lamin C-5A (mC-LC-5A) by infecting *LMNA*-KO HeLa cells with lentiviruses and observed that mC-LC-5A completely lost its ability to assemble the lamin C bodies under oxidative stress (Fig. 1J and 1K). The 5A mutant of Δ1BΔ2B59 (Δ1BΔ2B59-5A) also failed to form droplet-like condensates *in vitro* (Figs. S6D and S8D). Collectively, these data indicate that the positive charges provided by the arginine residues within the head domain promote the phase separation of lamin C proteins.

When we explored the regulatory mechanisms for the dynamics of lamin C bodies, we found that lamin C bodies formed by overexpression disassembled during mitosis, akin to the disassembly of the NL induced by the phosphorylation of lamin proteins, and lamin C bodies gradually disassembled upon removal of oxidative stress (Fig. S9A–C). The mass spectrometry analysis revealed that the level of S22 phosphorylation (pS22) in lamin A/C, a canonical site for lamin A/C phosphorylation that regulates NL disassembly, was lower in cells treated with (Murray-Nerger and Cristea, 2021) H_2O_2 than in control cells (Fig. S9D). Furthermore, compared with those of the control cells (HBSS), the levels of pS22-lamin C decreased significantly in cells under oxidative stress (H_2O_2), but when the cells were transferred to fresh H_2O_2-free medium, the level of pS22-lamin C recovered rapidly

sample in each experiment. (F) Representative images of LCmC condensates before and after treatment with 5% 1,6-hexanediol (hex). Scale bar, 20 μm. (G) Representative images of the fluorescence intensity recovery of LCmC condensates after photobleaching. Scale bars, 5 μm and 1 μm (zoom). (H) Quantitative FRAP data from (G). Ten condensates were counted. Scale bar, 20 μm. (I) *In vitro* phase separation assay of GLC-Δ1BΔ2B59. Representative images of the protein at the indicated concentrations in solution (25 mmol/L Tris-HCl, pH 7.5, 3% glycerol, 150 mmol/L KCl) with or without 10% PEG. Scale bar, 10 μm. (J) Representative images of cells stably expressing mC-LA (red), mC-LC-WT (red), and mC-LC-5A (red) and treated with 250 μmol/L H_2O_2 or HBSS for 40 min. Scale bar, 20 μm. (K) Quantification of the frequency of cells with condensates in (J). The data are presented as the mean ± SEM from three independent experiments. One hundred cells were counted per sample in each experiment. GFP-lamin A (GLA), GFP-lamin C (GLC), lamin C-mClover (LCmC), mCherry-lamin A (mC-LA), mCherry-lamin C-WT (mC-LC-WT), and mCherry-lamin C-5A (mC-LC-5A).

(Fig. S9E). These findings suggest that the pS22 level of lamin C fluctuates with changes in the level of cellular oxidative stress and that phase separation of the lamin C protein may be regulated by S22 phosphorylation. We verified this result by mutating S22 to aspartic acid (S22D) to mimic phosphorylation at this site or to alanine (S22A) to mimic its nonphosphorylated status and overexpressed these proteins in cells. We found that S22 phosphorylation diminished the phase separation ability of lamin C, whereas S22 nonphosphorylation preserved the phase separation ability and that the nonphosphorylation of lamin C also prevented disassembly of the lamin C bodies during mitosis (Fig. S9F–H). Collectively, these results indicate that a reduced level of pS22-lamin C promotes lamin C body assembly under oxidative stress, whereas an increased level of pS22-lamin C promotes disassembly of lamin C bodies upon the removal of oxidative stress.

Next, we investigated the biological significance of the lamin C bodies. Through an EdU incorporation assay, we found that most of the WT and *LMNA*-KO HeLa cells treated with H_2O_2 presented a very weak EdU intensity (Fig. S10A–D), suggesting that DNA replication in both types of cells under this stress was almost completely stalled. When the cells were moved into H_2O_2-free medium, DNA replication gradually recovered (Fig. S10B–D). However, compared with WT HeLa cells, *LMNA*-KO HeLa cells presented slower DNA replication recovery, as indicated by lower ratios of cell numbers with a high EdU intensity during the indicated recovery processes (Fig. S10B–D). The results of the DNA fiber assay revealed that the DNA replication fork velocity in *LMNA*-KO HeLa cells during recovery was much slower than that in control cells (Fig. S10E and S10F). Collectively, these data indicate that lamin A/C enhances DNA replication recovery upon removal of oxidative stress.

We assessed the roles of the lamin C bodies in DNA replication recovery by performing rescue experiments for both lamin A and lamin C in *LMNA*-KO HeLa cells through the transient expression of GFP, GLC-WT, GLC-5A, or GLC-5A-FUSN (GFP-lamin C-5A fused with the N-terminus of FUS protein (FUSN)) in mC-LA cells. FUSN, the intrinsically disordered region of FUS, has been used to confirm the role of phase separation in protein function (Sun et al., 2021), and here, we confirmed that FUSN rescued the phase separation ability of GLC-5A (Fig. S11). Compared with GFP and GLC-5A expression, the expression of GLC-WT and GLC-5A-FUSN, both of which can form lamin C bodies, rescued the velocity of the DNA replication fork and promoted the recovery of DNA replication (Fig. 2A–D). These results indicate that the lamin C bodies retain the ability to restore DNA replication during oxidative stress.

Finally, we investigated the mechanisms by which lamin C bodies orchestrate the DNA replication recovery process after oxidative stress. Through rapid immunoprecipitation mass spectrometry and immunofluorescence labeling, we found that the DNA replication factors proliferating cell nuclear antigen (PCNA), RPA1, RPA2, DNA polymerase delta (POLD) catalytic subunit (POLD1) and DNA ligase 1 (LIG1); the antioxidants peroxiredoxin 1 (PRDX1), PRDX2 and PRDX6; and the classic lamin A/C binding proteins barrier-to-autointegration factor (BAF) and lamina-associated polypeptide 2 (LAP2) were enriched in the lamin C bodies (Figs. 2E, 2F and S12A–D). Through a coimmunoprecipitation assay, we confirmed that lamin A/C interacted with these proteins under both control and oxidative stress conditions (Fig. S13), indicating that these proteins were recruited into the lamin C bodies via interactions with lamin A/C. Based on these results, we speculated that lamin C bodies might protect DNA replication factors from the impairment of oxidative stress by clustering them together with antioxidant proteins, and that the disassembly of lamin C bodies upon the removal of oxidative stress might promote the recovery of DNA replication through releasing DNA replication factors. To verify this, we assessed the interaction between PCNA and POLD1, a crucial interaction for the facilitation of DNA replication (Punchihewa et al., 2012), in S-phase cells after oxidative stress using a proximity ligation assay (PLA) (Fig. 2G). We observed that, compared with that in the control condition (HBSS-R2h), the PCNA–POLD1 interaction in the DNA replication recovery process (H_2O_2-R2h) was reduced in both the WT and *LMNA*-KO HeLa cells and that the PCNA–POLD1 interaction in *LMNA*-KO HeLa cells was weaker than that in WT HeLa cells under both HBSS-R2h and H_2O_2-R2h conditions (Fig. 2G and 2H). More importantly, compared with that under HBSS-R2h conditions, the degree of the decrease in the PCNA–POLD1 interaction under H_2O_2-R2h conditions was significantly greater in *LMNA*-KO HeLa cells than in WT HeLa cells (Fig. 2H). These results indicate that oxidative stress impairs the PCNA–POLD1 interaction and that lamin A/C may weaken this impairment. Through the PLA assay with mC-LA cells transiently expressing different lamin C proteins, we found that the expression of both FLAG-TagBFP-lamin C-WT (FBLC-WT) and FLAG-TagBFP-lamin C-5A-FUSN (FBLC-5A-FUSN) reversed the decrease in the PCNA–POLD1 interaction during the DNA replication recovery process, whereas the expression of both FLAG-TagBFP and FLAG-TagBFP-lamin C-5A (FBLC-5A) did not (Fig. 2I and 2J). These results indicate that lamin C may weaken the impairment of the PCNA–POLD1 interaction induced by oxidative stress by forming lamin C bodies.

Based on these results, we propose a working model to elucidate the roles of lamin C during oxidative stress (Fig. S14). Under oxidative stress, lamin C in the nucleus undergoes phase separation to assemble the lamin C bodies in response to stress. During this process, lamin C binds to DNA replication factors and antioxidants to

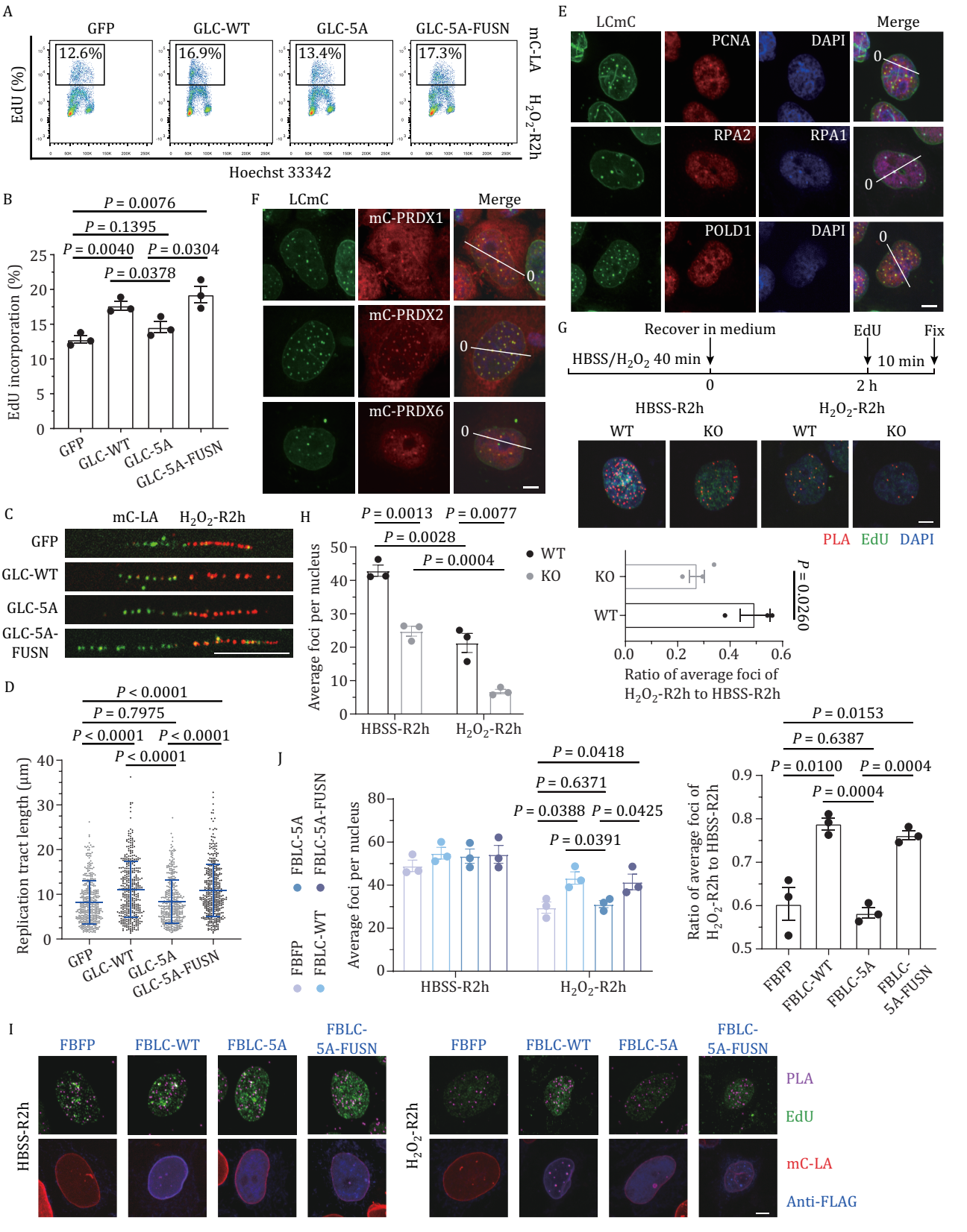

Figure 2. Lamin C bodies preserve the interaction between POLD1 and PCNA under oxidative stress and promote DNA replication recovery after oxidative stress. (A) Flow cytometry analysis of EdU incorporation in mC-LA cells transiently expressing GFP, GLC-WT, GLC-5A, or GLC-5A-FUSN under H_2O_2-R2h conditions. The experimental process is shown in Fig. S10A. The x-axis represents the DNA content indicated by Hoechst 33342 staining, and the y-axis represents the EdU intensity. The numbers represent the percentage of cells (high EdU intensity) in the corresponding boxes. (B) Quantification of the percentage of cells with a high EdU intensity in (A). The data are presented as the mean ± SEM from three independent experiments. (C and D) DNA fiber assay for stable mC-LA-transfected cells transiently expressing GFP, GLC-WT, GLC-5A, or GLC-5A-FUSN under H_2O_2-R2h conditions. The experimental process is shown

promote their accumulation in lamin C bodies to protect DNA replication factors during oxidative stress. Upon the removal of oxidative stress, the lamin C bodies gradually disassemble, releasing DNA replication factors for the recovery of DNA replication. DNA replication errors, stalls, and even damage frequently occur in cells under oxidative stress, and in response, these cells may quickly inhibit DNA replication initiation (Davalli et al., 2018; Fragkos et al., 2015), leading to the entry of DNA replication factors into an idle state, during which these factors need to be properly managed for later rapid use upon the removal of oxidative stress. We found that the lamin C bodies induced by oxidative stress provide temporary storage sites for DNA replication factors and protect them by concentrating them and antioxidants within gel-like condensates. Antioxidants within lamin C bodies may be able to remove ROS more efficiently and weaken the ability of ROS to impair DNA replication factors. More importantly, the assembly/disassembly cycle of lamin C bodies in response to the cellular redox status fits the dynamic regulatory needs of DNA replication factors well, temporarily and protectively storing these factors during oxidative stress, or releasing them in a timely manner to participate in DNA replication recovery once stress is relieved.

In summary, for the first time, in this work, we report that endogenous lamin C proteins are able to assemble condensates via phase separation and reveal a crucial function of lamin C condensates in the protection of DNA replication factors during oxidative stress. In addition to storing DNA replication factors, lamin C bodies may also enrich and safeguard other factors and regulators of relevant metabolic pathways during oxidative stress for use in the cell recovery process upon the removal of oxidative stress. Overall, this work provides significant implications for understanding the cellular responses to both intrinsic and extrinsic stressors, although a more complete physiological regulatory framework underlying the phase separation of lamin C to form lamin C bodies remains to be elucidated.

Supplementary data

Supplementary data is available at *Protein & Cell* online https://doi.org/10.1093/procel/pwaf016.

Footnotes

We thank Dr. Jing Yi (Shanghai Jiao Tong University) for providing the lentivirus plasmids and Dr. Jianguo Chen (Peking University) for providing the TagBFP plasmid. We thank the National Center for Protein Sciences at Peking University for assistance with flow cytometry and mass spectrometry and particularly thank Drs. Hongxia Lv, Jia Luo, Huan Yang, Xuefang Zhang, and Dong Liu for their technical support with related assays. We thank the Core Facilities at the School of Life Sciences, Peking University, for assistance with microscopy and the cDNA library and particularly thank Drs. Chunyan Shan, Siying Qin, Jun Ren, and Guilan Li for their technical assistance with related assays.

This work was funded by grants from the National Natural Science Foundation of China (92254305 and 32130026).

M.J. and C.Z. designed the experiments; M.J. analyzed the data and performed most of the experiments; G.Z., M.S., X.W., H.R., and G.X. performed some of the experiments; C.Z. supervised the project; and M.J., C.Z., and Q.J. wrote the manuscript.

Mingkang Jia, Gan Zhao, Mengjie Sun, Xiangyang Wang, He Ren, Guangwei Xin, Qing Jiang, and Chuanmao

in Fig. S10E. (C) Representative images of DNA fibers. Scale bar, 10 μm. (D) Quantification of the replication tract lengths in (C). Data points (n > 390 tracts per condition from two independent experiments) and mean ± SD are plotted. (E) DNA replication factors are concentrated in lamin C bodies. LAO-LCmC HeLa cells treated with 250 μmol/L H_2O_2 for 40 min were stained with anti-PCNA/DAPI, anti-RPA2/anti-RPA1 or anti-POLD1 /DAPI antibodies. Scale bar, 5 μm. (F) PRDXs are concentrated in lamin C bodies. LAO-LCmC HeLa cells transiently expressing mCherry-PRDX1, 2, or 6 (red) were treated with 250 μmol/L H_2O_2 for 40 min. DAPI (blue). Scale bar, 5 μm. (G and H) The interaction between PCNA and POLD1 was weaker in *LMNA*-KO HeLa cells than in WT HeLa cells. The experimental process is shown in Fig. S10A. The cells that recovered for 2 h were labeled with EdU (green) for 10 min, after which the PLA (red) assay was performed. DAPI (blue). (G) Scheme and representative images of the experiment. Scale bar, 5 μm. (H) Quantification of the average number of foci per nucleus in (G) and the ratio of the average number of foci per nucleus in cells treated with H_2O_2-R2h condition to those in cells treated with HBSS-R2h condition. Only the EdU-positive (S phase) cells were counted. The data are presented as the mean ± SEM from three independent experiments. More than 50 cells were counted per sample in each experiment. (I and J) PLA of cells stably expressing mC-LA (red) and transiently transfected with FBFP, FBLC-WT, FBLC-5A, or FBLC-5A-FUSN under the indicated conditions. The experimental process is shown in (G), and after EdU labeling (green) and the PLA (magenta), the cells were stained with an anti-FLAG antibody (blue). (I) Representative images of the PLA. Scale bar, 5 μm. (J) Quantification of the average number of foci per nucleus in (I) and the ratio of the average number of foci per nucleus in cells treated with H_2O_2-R2h condition to those in cells treated with HBSS-R2h condition. For FBLC-WT, 5A, and 5A-FUSN, EdU- and FLAG-double-positive cells were counted, whereas, for FBFP, only EdU-positive (S phase) cells were counted, as BFP cannot be fixed with methanol. The data are presented as the mean ± SEM from three independent experiments. More than 35 cells were counted per sample in each experiment. GFP-lamin C (GLC), recovered after 2 h (R2h), mCherry-lamin A (mC-LA), lamin C-mClover (LCmC), FLAG-TagBFP (FBFP), FLAG-TagBFP-lamin C-WT (FBLC-WT), FLAG-TagBFP-lamin C-5A (FBLC-5A), and FLAG-TagBFP-lamin C-5A-FUSN (FBLC-5A-FUSN).

Zhang declare that they have no conflicts of interest. The authors declare their agreement to participate and to publish.

All pertinent data are provided in the main text and Supplemental Materials. A list of the reagents included in this study is available upon request from the corresponding author.

References

Burke B, Stewart CL. The nuclear lamins: flexibility in function. *Nat Rev Mol Cell Biol* 2013;**14**:13–24.

Davalli P, Marverti G, Lauriola A *et al*. Targeting oxidatively induced DNA damage response in cancer: opportunities for novel cancer therapies. *Oxid Med Cell Longev* 2018;**2018**:2389523.

Fragkos M, Ganier O, Coulombe P *et al*. DNA replication origin activation in space and time. *Nat Rev Mol Cell Biol* 2015;**16**:360–374.

Guillén-Boixet J, Kopach A, Holehouse AS *et al*. RNA-induced conformational switching and clustering of G3BP drive stress granule assembly by condensation. *Cell* 2020;**181**:346–361.

Izumi M, Vaughan OA, Hutchison CJ *et al*. Head and/or CaaX domain deletions of lamin proteins disrupt preformed lamin A and C but not lamin B structure in mammalian cells. *Mol Biol Cell* 2000;**11**:4323–4337.

Murray-Nerger LA, Cristea IM. Lamin post-translational modifications: emerging toggles of nuclear organization and function. *Trends Biochem Sci* 2021;**46**:832–847.

Punchihewa C, Inoue A, Hishiki A *et al*. Identification of small molecule proliferating cell nuclear antigen (PCNA) inhibitor that disrupts interactions with PIP-box proteins and inhibits DNA replication. *J Biol Chem* 2012;**287**:14289–14300.

Sies H, Jones DP. Reactive oxygen species (ROS) as pleiotropic physiological signalling agents. *Nat Rev Mol Cell Biol* 2020;**21**:363–383.

Somyajit K, Gupta R, Sedlackova H *et al*. Redox-sensitive alteration of replisome architecture safeguards genome integrity. *Science* 2017;**358**:797–802.

Sun M, Jia M, Ren H *et al*. NuMA regulates mitotic spindle assembly, structural dynamics, and function via phase separation. *Nat Commun* 2021;**12**:7157.

Sylvius N, Bilinska ZT, Veinot JP *et al*. *In vivo* and *in vitro* examination of the functional significances of novel lamin gene mutations in heart failure patients. *J Med Genet* 2005;**42**:639–647.

Sylvius N, Hathaway A, Boudreau E *et al*. Specific contribution of lamin A and lamin C in the development of laminopathies. *Exp Cell Res* 2008;**314**:2362–2375.

Thor H, Smith MT, Hartzell P *et al*. The metabolism of menadione (2-methyl-1,4-naphthoquinone) by isolated hepatocytes. A study of the implications of oxidative stress in intact cells. *J Biol Chem* 1982;**257**:12419–12425.

Valois E, Mirshafian R, Waite JH. Phase-dependent redox insulation in mussel adhesion. *Sci Adv* 2020;**6**:eaaz6486.

Wang L, Yang W, Li B *et al*. Response to stress in biological disorders: Implications of stress granule assembly and function. *Cell Prolif* 2021;**54**:e13086.

Wilhelm T, Ragu S, Magdalou I *et al*. Slow replication fork velocity of homologous recombination-defective cells results from endogenous oxidative stress. *PLoS Genet* 2016;**12**:e1006007.